Magnetoresistance and Anomalous Hall Effect of InSb Doped with Mn

A.V. Kochura[1,2,*], B.A. Aronzon[2,3], M. Alam[1], A. Lashkul[2], S.F. Marenkin[4], M.A. Shakhov[2,5],
E.P. Kochura[1], E. Lahderanta[2]

[1] *Southwest State University, 94, 50 Let Oktjabrja Str., 305040 Kursk, Russia*
[2] *Laboratory of Physics, Lappeenranta University of Technology, PO Box 20, FIN-53851, Lappeenranta, Finland*
[3] *Russian Research Centre "Kurchatov institute", 1 Kurchatov Sq., 123182 Moscow, Russia*
[4] *Institute of General and Inorganic Chemistry of Russian Academy of Sciences, 31, Leninskii Pr.,
119991 Moscow, Russia*
[5] *Ioffe Physical Technical Institute, 26, Polytekhnicheskaya Str., 194021 St.-Petersburg, Russia*

Transport properties of polycrystalline (In, Mn)Sb samples are investigated. Behavior of the temperature and magnetic field dependencies of the resistivity, anomalous Hall coefficient and magnetoresistivity at low temperatures points out the influence of Mn complexes, Mn ions and nano- and microsizes MnSb precipitates on charge transport.

Keywords: Spintronic materials, Indium antimonide, Magnetoresistivity, Anomalous Hall effect, Spin-dependent scattering, Nanoclusters.

PACS numbers: 72.20.Dp, 75.50.Dd, 72.20.My

1. INTRODUCTION

Alloying of nonmagnetic semiconductors with 3d-magnetic elements can be used to synthesize diluted magnetic semiconductors (DMS). Progress in the investigation of Mn doped III-V DMS has shown high potential for spintronics applications,[1] but their ferromagnetic Curie temperatures ($T_C \approx 200$ K for $Ga_{1-x}Mn_xAs$) [2] do not reach room temperature as required in traditional electronic devices. Better results are expected by doping non-magnetic semiconductors with ferromagnetic Mn-V compounds such as MnAs (in zero magnetic field $Tc = 317$ K) [3] and MnSb ($Tc = 585$ K) [4]. Hysteresis character of anomalous Hall effect was observed in (Ga, Mn)Sb films containing MnSb clusters even above the room temperature and depended on hole concentration.[5] It point to that the ferromagnetic (FM) signal in (Ga, Mn)Sb films is produced not only by non-interactingMnSb clusters.

Ferromagnetic (FM) $In_{1-x}Mn_xSb$ films with T_C reaching 20 K [6] were grown by low-temperature molecular-beam epitaxy. The detailed studies of such structures showed that FM state in this case is carrier mediated, it demonstrate itself in charge transport properties and is related to Mn atoms substituting In.[7, 8] Accurate theoretical mean-field calculations predict the existence of ferromagnetic $In_{0.95}Mn_{0.05}Sb$ with $Tc < 40$ K and itinerant hole density $p = 5 \cdot 10^{20}$ cm^{-3}. [9]

However Curie transitions above room temperature were observed in InSb:Mn films and bulk polycrystalls grown by different methods.[10-13] But, experiments have shown that high-temperature ferromagnetism in heavily Mn doped InSb is not hole-mediated and is caused by noninteracting MnSb clusters.[10-14]. Another source of magnetic properties in InSb:Mn are magnetically active atomic scale complexes resulting from correlation in special distribution of Mn atoms placed In positions [15]. Theoretical calculations performed for (Ga,Mn)As system showed possibility of Mn clustering into stable and electronically active dimmer, trimer or tetramer.[16]

The aim of this paper is to investigate the role of various origins of FM (Mn atoms substituted cation sites, MnSb grains and atomic scale magnetic complexes) in forming of magnetoelectrical properties of InSb:Mn prepared by solid state reaction with fast cooling rate at nonequilibrium conditions.

2. EXPERIMENTAL DETAILS

Direct melting of indium antimonide with manganese and antimony was used to syntheses polycrystalline InMnSb samples as it described in [12]. The starting materials were single crystal n-type InSb ($n = 3 \cdot 10^{15}$ cm^{-3}, $\mu_n > 4 \cdot 10^5$ cm^2/(V·s) at $T = 77$ K), high purity antimony (5N) and bisublimed manganese (4N). The samples were synthesized in evacuated quartz ampules, which were coated with pyrolytic graphite. The synthesis was performed at temperature 1050 K during 24 h. This temperature exceed the InSb melting temperature (800 K) to make conditions for better homogenization of the melt. To reach the maximal solubility of manganese in InSb the final step of growing procedure was fast cooling (cooling rate 10-12 K/s) of ampules. This non equilibrium growth method was chose to exceed the solubility limit of Mn in bulk InSb$5 \cdot 10^{18}$-$1 \cdot 10^{19}$ cm^{-3} at equilibrium growth [17] and reach solubilutybelow 10^{20} cm^{-3} [14]. Prepared samples contained 0.47; 0.7 and 1.42 mas. % of Mn and labeled as #A1, #A2, and #A3, respectively.

The composition and structure of the crystals were studied by atomic absorption analysis, atomic force (AFM) and electronic scanning (SEM) microscopy and described in [14] in detail.

The electrical and magnetotransport properties of samples were investigated between 1.6 K and 320 K

---

*akochura@mail.ru

using the standard six-point geometry, where the four side contacts allow the simultaneous measurement of the longitudinal and the transverse voltage. The samples with the dimensions $5 \times 1 \times 0.1$ mm^3 were cut from crystals. Contacts to samples were prepared by soldering of tin-and-leaden solder.

The pulse solenoid was used to generate the pulse magnetic field up to 150 kG with the pulse duration about 10 ms. Sample #A3 was investigated additionally with dc superconducting solenoid in magnetic field up to 70 kG at 1.6 К and 3.5 К. In all measurements the magnetic field was applied perpendicularly to the biggest face of sample. The resistance was measured with a high accuracy (the error was at most 1 % of the measured value). The samples had high conductivity of *p*-type and linear current-voltage characteristics in the range of the measurements.

3. RESULTS AND DISCUSSION

SEM investigations showed that the samples grown under non equilibrium conditions contained clusters which correspond to the three-dimensional microcrystalline MnSb (Fig. 1) and have granular structure [14]. The lateral size of these clusters ranges mainly from 100 to 600 nm. The structure of one of these clusters was investigated in [14] and shown that sample #A3 has fine structure and is composed from nanograins with a mean size about 24 nm and Gauss-like distribution of the nanograin diameter. Similar structure of InSb:Mn alloys was also observed and described in [18].
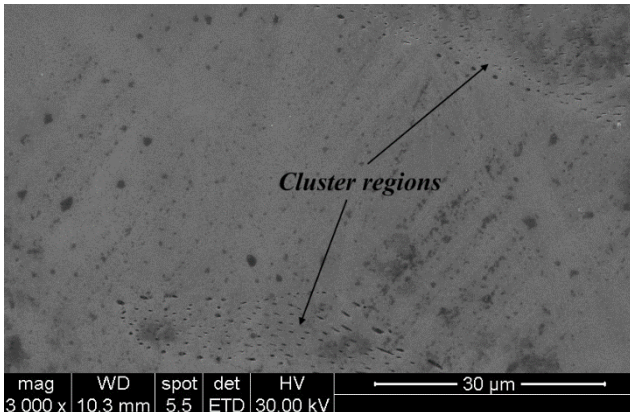

Fig. 1 – SEM images of InSb:Mn sample #A3 demonstrated precipitated clusters of Mn-Sb phase

Energy dispersive analyze showed that the clusters in InSb:Mn samples are formed by Mn-Sb phases. Additional phases were not detected accurately because of two reasons. The first is small size of clusters. The electron beam penetration exceeds the mean diameter of a cluster. Therefore the peaks of matrix atoms were observed on dispersive curves together with cluster atoms, and quantitative analysis of cluster composition is not possible. Second, for MnSb, there is a problem of nonstoichiometry, which comes from the phase stability of the NiAs structure in the binary phase diagram of the Mn-Sb system [19]. For example Mn content x in the $Mn_{1+x}Sb$ compounds can change from 0 up to 0.28 [20].

Finally structure and magnetic [14] studies demonstrate the existence of Mn entered In position forming the $In_{1-x}Mn_xSb$ matrix with MnSb grains embedded in it.

3.1 Resistivity

To investigate the contribution of Mn atoms substituting In cites inside the $In_{1-x}Mn_xSb$ matrix to electrical properties we have studied magnetotransport properties of our polycrystalline InSb:Mn samples. Fig. 2 shows the sample resistivity $\rho(T)$ in the range of 1.6-30 K. At higher temperatures up to 300 K the smooth increase of the resistivity was observed as it was reported earlier.[12] All $\rho(T)$ curves presented in Fig. 2 (inset a), demonstrate a minimum at $T \approx 10\text{-}15$ K which is related to crossover from metallic to hopping conductivity at lower temperatures.
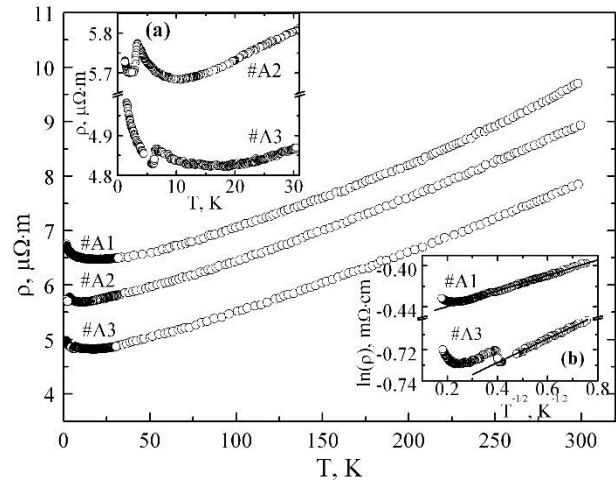
Fig. 2 – Temperature dependences of zero-field resistivity ρ for InSb:Mn samples. The inset (a) demonstrate low-temperature peaks occurring near ferromagnetic transition. Inset (b) show the lnρ vs $T^{-1/2}$ for samples #A1 and #A2

The hopping type of conductivity at low temperatures is proved by plots lnρvs. $T^{-1/2}$ shown in Fig. 1, inset (b). This is the best fit for T^{-m}type functions at temperatures below 10 K. $m = 1/2$ is typical for conductivity for the variable range-hopping regime with Culomb gap in the density of electron states as it was predicted by Shklovskii and Efros [21]. According to the Zvyagin and Keiper model [22] the $T^{-1/2}$ law is valid also for granular materials due to variable range hopping of carriers between grains located far away from each other. It is suggested that the intergranular electron transport involves transitions to virtual states, since direct transitions are extremely improbable in the range of temperatures of the experiment. However, the hopping through states inside the impurity band is much more probable than hopping between MnSb grains because their concentration is very small.

One of the main features of the data presented in Fig. 2, inset (a) is the peak observed in $\rho(T)$ dependencies for the samples #A2 and #A3. Such behavior is the sign of FM transition and it is widely used for T_c determination [23]. It is important to note that the existence of this peak in the vicinity of the Curie temperatureand similar behavior of $\rho(T)$ was also found in ferromagnetic $In_{1-x}Mn_xSb$ films grown by MBE [7, 8] with the similar values of the Curie temperatures. In our samples the peak of $\rho(T)$ dependence could be attributed to the ferromagnetic transition inside the $In_{1-x}Mn_xSb$ matrix with $T_{Cm} \approx 3$ K in #3 and $T_{Cm} \approx 6$ K in #A3,

where T_{Cm} is the temperature of this transition. The non-monotonic behavior of $\rho(T)$ near T_C in DMS is usually associated with giant magnetoresistance (GMR) effect [23] or with critical scattering as predicted by the scaling theory of magnetotransport in Anderson localized disordered ferromagnets due to interplay between magnetism and disorder near the magnetic phase transition.[24] For our case the matter is that the FM transition occurs in the range of hopping conductivity when there are no free electrons for Ruderman-Kittel-Kasuya-Yosida exchange mechanism. However, it is not something new and surprising. The FM ordering under insulating regime were already discussed in various materials [25], while reasons for the non-monotonic $\rho(T)$ behavior are the same as in metallic samples if instead of GMR the tunneling magnetoresistance will be taken into account. It should be mentioned that both magnetization and transport properties observed in Ge:Mn [26, 27] are very similar to those revealed in our samples. The nature of the exchange in samples with nonmetallic conductivity is discussed and related to carriers localized in the impurity band or to the bound magnetic polaron percolation model of ferromagnetism [26, 27].

3.2 Hall Effect

The magnetization in our samples manifests itself also as anomalous Hall effect.

It is well known that the Hall resistivity of magnetic materials can be expressed by a sum of two terms,

$$\rho_H = R_{0H}H + R_{aH}M = \rho_{oH} + \rho_{aH} \qquad (1)$$

where R_{0H} and R_{aH} are the normal and the anomalous Hall coefficients, respectively. The normal Hall resistivity ρ_{0H} is caused by the Lorentz force while the anomalous part ρ_{aH} is proportional to M and tends to saturation in ferromagnetic materials at high magnetic fields. The anomalous Hall coefficient depends on the longitudinal resistivity as

$$R_{oH} \propto \rho^{n}, \qquad (2)$$

where $n = 1$ in the case of skew-scattering or 2 for the side-jump scattering and the intrinsic (Berry phase) mechanism [23]. Subtracting the contribution $\rho_{oH}(H)$ (which is very close to linear for $In_{1-x}Mn_xSb$) [28] from the total Hall resistivity ρ_H we get $\rho_{aH}(H)$. The ρ_H data obtained for sample #A1 are shown in Fig. 3 where the anomalous contribution ρ_{aH} is displayed in the inset. In this sample the anomalous Hall effect (AHE) is observed even with not high Mn content and when the $\rho(T)$ dependence does not demonstrate the peak related to FM transition at low temperatures. Temperature dependences $M(T)$ is opposite to $\rho_H(T)$. Magnetization is decreasing and ρ_H is increasing with increasing of temperature. That could be due to increase of the carrier concentration or due to crossover from hopping conductivity to conductivity along the percolation pass. Also it is seen from eq. (2) because ρ increases with increasing of temperature (see Fig. 2). AHE saturates at magnetic field which exceed the saturation field of magnetization by one order of magni-

tude due to shape anisotropy of the sample because AHE measurements were performed in fields perpendicular to the sample plane while magnetization was measured in fields oriented along the sample.
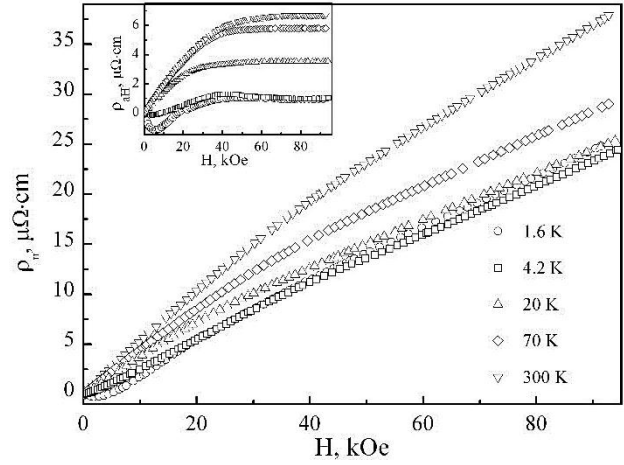
Fig. 3 – Hall resistivity ρ_H of sample #A1 measured at various temperatures in fields up to $H = 95$ kOe. Inset illustrates the field dependences of the anomalous Hall resistivity ρ_{AH} at various temperatures
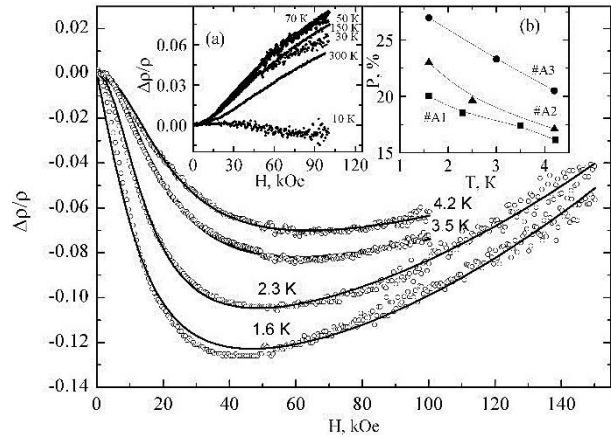
Fig. 4 – Magnetic field dependence of the magnetoresistance for sample #A1 at low temperatures measured in pulsed magnetic fields. Inset (a) show Magnetic field dependence of the magnetoresistance for sample #A1 at T > 10 K. Inset (b) show spin polarization of InSb:Mn samples at low temperatures

As shown in Fig. 3, in weak magnetic fields AHE is predominant, while at high fields ρ_H is linear due to the saturation of the AHE term. The behavior of $\rho_{aH}(H)$ is nonmonotonic at low temperatures and similar to that observed $In_{1-x}Mn_xSb$ epitaxial films, [28] characterized by a shallow minimum and a sign reversal below 40 kOe leading to saturation in high magnetic fields. Such trend was explained within intrinsic (Berry-phase) mechanism of AHE [28]. However, we believe that such behavior (negative derivative of $\rho_{aH}(H)$ at low temperatures and small fields) rather is related to quantum corrections of conductivity, [29] which is natural for such conditions.

3.3 Magnetoresistance

The magnetoresistance $\Delta\rho/\rho = [\rho(H) - \rho(0)]/\rho(0)$ of samples #A1 is shown in Fig. 4 at different temperatures. Here $\rho(H)$ and $\rho(0)$ are the sample resistivity in magnetic field H and in zero magnetic field, respectively. The main feature of these curves is the negative magnetoresistance which is observed at low temperatures and even in high enough magnetic fields. At higher magnetic fields or temperatures it changes by the traditional, classic positive magnetoresistance. There are two reasons for negative magnetoresistance: quantum corrections to conductivity [29] and the magnetic nature (spin dependent scattering or tunneling of carriers). The existence of the quantum corrections contribution to the negative magnetoresistance is witnessed by the observation of positive magnetoresistance at very small fields which is seen at Fig. 4, inset (a) and is due to strong spin-orbit interaction [29]. However we will not pay too much attention to this contribution because the negative magnetoresistance takes place at very high magnetic fields and we believe that in magnetic semiconductor spin dependent scattering or tunneling should play a main role. Maximum negative magnetoresistance $\Delta\rho/\rho - 16.3\%$ at $T = 1.6$ K is observed in sample #A3 . At $T < 10$ K $\Delta\rho/\rho$ is negative up to 40-90 kOe and has an upturn due to a positive contribution in increasing magnetic fields.

The origin of the negative magnetoresistance in heavily Mn-doped InSb at low temperatures may be the spin-dependent scattering of carriers by isolated Mn^{2+} ions and magnetic Mn complexes or tunneling probability for parallel- and antiparallel oriented spins of carries and magnetic moments embedded in matrix. The amount of the antiparallel particles diminishes with magnetic field leading to a decrease of the resistivity. In the range of $T < T_{Cm}$ the volume of the ferromagnetically ordered regions in the matrix increases but some Mn^{2+} spins can still remain outside the ferromagnetic network and the magnetoresistance is proportional both to spin polarization P arising from the ferromagnetic regions and to ordering of the isolated paramagnetic moments, [30]

$$\frac{\Delta\rho}{\rho} = -4P\frac{J_{pd}}{V}\langle S_Z \rangle = -4P\frac{J_{pd}}{g\mu_B V}M(H), \qquad (3)$$

Here J_{pd} is the coupling constant, V is the spin-independent part of the Hamiltonian for interaction between delocalized holes and the $3d$ shells of the Mn^{2+} ions, μ_B is the Bohr magneton, and $<S_z>$ is given by the Brillouin function $B_{5/2}(a)$ with argument $a = (g\mu_B H) = k_B T_{eff}$ with $T_{eff} = T + T_{AF}$, where T_{AF} is the empirical antiferromagnetic coupling parameter. For epitaxial InMnSb films the values of $J_{pd}/V \approx 0.17$ and $T_{AF} = 1.4$ K were observed earlier in [30]. Using the eq. (3) for fitting of experimental $\Delta\rho/\rho(H)$ dependencies we can found spin polarization vs. temperature $P(T)$ (Fig. 4, inset (b)) for InSb:Mn samples. Before the fitting procedure the quadratic classical contribution to $\Delta\rho/\rho(H)$ be estimated from high field part of

$\Delta\rho/\rho(H)$ curve, as at high magnetic fields the negative contribution of $\Delta\rho/\rho(H) \sim B_{5/2}(a)$ is close to saturation.

At $T > T_c$, the ferromagnetic phase becomes paramagnetic and the magnetoresistance is expressed by [30]

$$\frac{\Delta\rho}{\rho} = -\frac{J_{pd}^2}{V^2}\left[4\langle S_z \rangle^2 + \langle S_z \rangle\left(\coth\frac{\alpha}{2} - \frac{\alpha}{2\sinh^2\frac{\alpha}{2}}\right)\right], \quad (4)$$

with $T_{eff} = T - T^*$, where T^* is usually close to T_C. When the ferromagnetic ordering changes to paramagnetic the dependence of $\Delta\rho/\rho$ on $\langle S_z \rangle$ becomes quadratic.

Second reason for the negative magnetoresistnce in our case could be related to the magnetic MnSb clusters similar to the approach suggested for granular paramagnetic-ferromagnetic GaAs:Mn / MnAs hybrid layers with nano-scaled MnAs clusters embedded in the GaAs:Mn matrix [31]. In general, the magnetoresistance in these systems is controlled by competition of the negative and positive terms while the paramagnetic matrix plays a significant role.

When the temperature increasing, the negative magnetoresistance decreases rapidly and becomes positive reaching a maximum $\Delta\rho/\rho = 8.4\%$ at $T \approx 70$ K for sample #4 and then slowly decreases. The similar behavior was observed for (In, Mn)Sb crystals containing MnSb micro clusters [11] and for GaAs:Mn / MnAs [31], where the value of $\Delta\rho/\rho$ depends on both the size and distribution of the clusters in the matrix.

Both above mechanisms are important for the negative magnetoresistance in our samples. However, the concentration of MnSb clusters in our case is much smaller than manganese concentration and hole concentration being about $2 \cdot 10^{15}$ cm^{-3} [14]. So their role for spin dependent scattering or tunneling should be not important in compare to that described by eq. (3) and (4). This statement is also supported by the observation that the negative magnetoresistance takes place only at temperatures lower or close to T_{Cm} related to the FM transition in the $In_{1-x}Mn_xSb$ matrix, where all magnetic moments tend to be parallel. So we assume that for negative magnetoresistance the main contribution at low temperatures is coming from the spin-dependent scattering or tunneling of carriers between magnetic moments inside matrix. Because the main mechanism of a conductivity in this temperature range is hopping the spin-dependent tunneling should dominate as the reason for negative magnetoresistance. According eq. (3) and (4) $\Delta\rho/\rho \sim M$ for FM state and $\Delta\rho/\rho \sim M^2$ for paramagnetic state. Here we believed that $\langle S_z \rangle$ is proprional to M. Taking that into account we can estimate the temperature dependence of magnetization $M_{eff}(T)$ obtained from the $\Delta\rho/\rho(T)$ at low temperatures, for that the positive magnetoresistance was subtracted because it weakly depends on temperature in the range 30-150 K as it is seen from Fig. 4, inset(a). It should be mentioned that calculated $M_{eff}(T)$ value is related to the magnetization caused by the
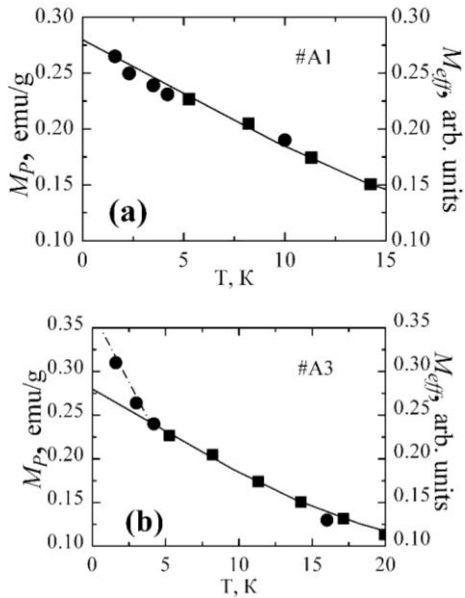
Fig. 5 – Temperature dependences of magnetizations InSb:Mn samples #A1 (a) and #A3 (b) in magnetic field $H = 50$ kOe. The contribution of MnSb inclusions was removed. M_p data (squares) were taken from [14]. M_{eff} (circles) were calculated from Hall measurements on conditions that $\Delta\rho/\rho \sim M$ for the ferromagnetic and $\sim M^2$ for the paramagnetic states. Continuous lines are interpolation of the M_p data. For sample #A3 circles are situated beyond of paramagnetic line. It point out on presence of the transition to the ferromagnetic state

magnetic moments inside the $In_{1-x}Mn_xSb$ matrix, but does not take into account the magnetization of big MnSb clusters. It is relevant to the assumption that these clusters do not contribute essentially to the negative magnetoresistance. The results of $M_{eff}(T)$ calculations are presented in Fig. 5 for samples #A1 and #A3. It is seen that for sample #A1 (Fig. 5a) the obtained $M_{eff}(T)$ coincide with $M_p(T)$ which is the calculated paramagnetic contribution to $M(T)$ obtained from the magnetometry data taking from Ref. [14], while for sample #A3 $M_{eff}(T)$ deviate at $T < T_{Cm}$ from this interpolation to higher values. That is in agreement with observation of

low-temperature peak at $\rho(T)$ for the sample #A3 (Fig. 2, inset (a)) and its absence for the sample #A1, which proves the FM transition but only for sample #A3 (Fig. 5b).

4. CONCLUSION

In summary, we have investigated the structural, and electrical properties of polycrystalline (In, Mn)Sb with different Mn contents. We have observed the anomalous Hall effect up to room temperature, positive magnetoresistance about 6 % at $T = 300$ K, FM transition in the $In_{1-x}Mn_xSb$ matrix and negative magnetoresistance at $T < 10$ K. Maximal spin polarization is close to 30 % at low temperatures. From the above presented results we can conclude that following inclusions contribute to magnetization and magnetotransport in (In, Mn)Sb and succeed to find out contributions of each of them to magnetization and magnetotransport observed:

MnSb clusters are responsible for high temperature positive magnetoresistance and Hall effect. These inclusions with inhomogeneous spatial distribution have sizes up to 500 nm;

Mn complexes, mainly dimmers formed fromMn ions, substituting In in the $In_{1-x}Mn_xSb$ matrix,are responsible for the paramagnetic background and for FM transition in matrix at $T < 10$ K.

In bulk (In, Mn)Sb the majority of Mn atoms are located in MnSb nanoclusters. Analysis of the temperature and magnetic field dependencies of the resistivity, anomalous Hall coefficient and the magnetoresistivity shows that the ferromagnetic MnSb nanoclusters and Mn ions influence significantly the charge transport in the investigated materials.

REFERENCES

1. T. Dietl, *Nat. Mater.* **9**, 965 (2010).
2. L. Chen, X. Yang, F. Yang, J. Zhao, J. Misuraca, P. Xiong, S. von Molnar, *Nano.Lett.* **11**, 2584 (2011).
3. L. Pultik, A. Zieba, *J. Magn. Magn. Mater.* **51**, 199 (2005).
4. W.J. Takei, D.E. Cox, G. Shirane, *Phys. Rev.* **129**, 2008 (1963).
5. V.V. Rylkov, B.A. Aronzon, Yu.A. Danilov, Yu.N. Drozdov, V.P. Lesnikov, K.I. Maslakov, V.V. Podolskii, *JETP* **100**, 742 (2005).
6. S. Yanagi, K. Kuga, T. Slupinski, H. Munekata, *Physica E* **20**, 333 (2004).
7. T. Wojtowicz, G. Cywinski, W.L. Lim, X. Liu, M. Dobrowolska, J.K. Furduna, K.M. Yu, W. Walukiewicz, G.B. Kim, M. Cheon, X. Chen, S.M. Wang, H. Luo, *Appl. Phys. Lett.* **82**, 4310 (2003).
8. M. Csontos, G. Mihaly, B. Janko, T. Wojtowicz, X. Liu J.K. Furduna, *Nat. Mater.* **4**, 447 (2005).
9. T. Jungwirth, J. Konig, J. Sinova, A.H. MacDonald, *Phys. Rev. B* **66**, 012402 (2002).
10. C.E. Feeser, L. Lari, V.K. Lazarov, J.A. Peters, B.W. Wessels, *J. Vac. Sci. Technol. B* **30**, 032801 (2012).
11. K. Ganesan, H.L. Bhat, *J. Appl. Phys.* **103**, 043701 (2008).
12. V.M. Novotortsev, I.S. Zakharov, A.V. Kochura, S.F. Marenkin, R. Laiho, E. Lahderanta, A. Lashkul, A.G. Veresov, A.V. Molchanov, G.S. Yur'ev, *Russ. J. Inorg. Chem.* **51**, 1627 (2006).
13. V.A. Ivanov, O.N. Pashkova, E.A. Ugolkova, V.P. Sanygin, R.M. Galera, *Inorg. Mater.* **44**, 1041 (2008).
14. A.V. Kochura, B.A. Aronzon, K.G. Lisunov A.V. Lashkul, A.A. Sidorenko, R.De Renzi, S.F. Marenkin, M. Alam, A.P. Kuzmenko, E. Lahderanta, *J. Appl. Phys.* **113**, 083905 (2013).
15. N.D. Parashar, N. Rangaraju., V.K. Lazarov, S. Xie, B.W. Wessels, *Phys Rev B* **81**, 115321 (2010).
16. H. Raebiger, A. Ayuela, J. von Boehm, *Phys. Rev. B* **72**, 014465 (2005).
17. M.Y. Dashevskii, V.S. Ivleva, L.Y. Krol, I.N. Kurilenko, L.B. Litvak-Gorskaya, R.S. Mitrofanova, E.Y. Fridlyand,

Sov. Phys. Semicond. **5**, 757 (1971).
18. L. Rednic, I.G. Deac, E. Dorolti, M. Coldea, V. Rednic, M. Neumann, *Central Eur. J. Phys.* **8**, 620 (2010).
19. I. Teramoto, A.M.J.G. van Run, *J. Phys. Chem. Sol.* **29**, 347 (1968).
20. T. Chen, G.B. Charlan, R.C. Keezer, *J. Cryst. Growth* **37**, 29 (1977).
21. B.I. Shklovskii, A.L. Efros, *Electronic Properties of Doped Semiconductors* (Berlin: Springer, 1984).
22. I.P. Zvyagin, R. Keiper, *phys. status solidi (b),* **230**, 151 (2002).
23. T. Jungwirth, J. Sinova, J. Masek, J. Kucera, A.H. MacDonald, *Rev. Mod. Phys.* **78**, 809 (2006).
24. C.P. Moca, B.L. Sheu, N. Samarth,P. Schiffer, B. Janko, G. Zarand, *Phys. Rev. Lett.* **102**, 137203 (2009).
25. C.J. Timm, *J. Phys. Condens. Mater.* **15**, R1865 (2003).

26. A.P. Li, J. Shen, J.R. Thompson, H.H. Weitering, *Appl. Phys. Lett.* **86**, 152507 (2005).
27. R. Morgunov, M. Farle, M. Passacantando, L. Ottaviano, O. Kazakova, *Phys. Rev. B* **78**, 045206 (2008).
28. G. Mihaly, M. Csontos, S. Bordacs, I. Kezsmarki, T. Wojtowicz, X. Liu, B. Janko J.K. Furduna, *Phys. Rev. Lett.* **100,** 107201 (2008).
29. P.A. Lee, T.V. Ramakrishnan, *Rev. Mod. Phys.* **57**, 287 (1985).
30. M. Csontos, T. Wojtowicz, X. Liu, M. Dobrovolska, B. Janko, J.K. Furduna, G. Mihaly, *Phys. Rev. Lett.* **95**, 227203 (2005).
31. W. Heimbrodt, P.J. Klar, S. Ye, M. Lampalzer, C. Michel, S.D. Baranovskii, P. Thomas, W. Stolz, *J. Supercond.* **18**, 315 (2005).